sociedade & natureza

DOI: 10.14393/SN-v36-2024-72381x
Received: 05 February, 2024 | Accepted: 19 June, 2024 | Published: 12 September, 2024

Papers

Carbon Flux Models in a Zonally Dry Tropical Forest Area (Caatinga)

Joélia Natália Bezerra da Silva[1]
Rodrigo de Queiroga Miranda[2]
Gabriel Antônio Silva Soares[3]
Magna Soelma Beserra de Moura[4]
Josiclêda Domiciano Galvíncio[5]

Keywords
Remote sensing
Modeling
Semi-arid

Abstract
Studies on energy exchange in ecosystems are critical for understanding carbon flows amid different vegetation patterns. In semi-arid areas, comprehending the variability in carbon absorption is essential for quantifying and anticipating the impacts of changes in the caatinga ecosystem. This study aims to calibrate and evaluate models for Gross Primary Production (GPP), Net Ecosystem Exchange (NEE), and Ecosystem Respiration (Reco) in the caatinga biome. NEE measurements were obtained and calculated at 30-minute intervals using EddyPro 3.6 software, from raw data measured at 10 Hz. GPP was estimated by partitioning NEE and Reco, all measured in micromoles of CO_2 per square meter per second (µmol CO_2 m^{-2} s^{-1}) using the eddy covariance (EC) tower, installed in a legal reserve at Embrapa Semiárido, in Petrolina, Pernambuco, within a section of the caatinga canopy. Following the measurement of carbon fluxes and ecosystem respiration, field measurements were conducted using a portable FieldSpec HandHeld spectroradiometer to obtain the reflectance of the canopy around the turbulent eddy covariance tower. These measurements were carried out in 2015 in a preserved caatinga area. Multiple linear regression models were developed to estimate carbon fluxes from orbital images, enabling accurate estimation of GPP, NEE, and Reco, using the MODIS/Terra Daily Surface Reflectance product (MOD09GA). The primary results demonstrate the effectiveness of the developed models, particularly the GPP model, which exhibited the best statistical indices ($R = 0.97$; $R^2 = 0.95$; Root Mean Square Error = 0.20). Observations from the EC tower indicated that the models developed to estimate NEE, GPP, and Reco, using visible and near-infrared reflectance data, accurately represented the dry period and effectively captured the phenological aspects of the caatinga ecosystem.

[1] Universidade Federal de Pernambuco – UFPE, Recife, PE, Brazil. joelia.silva@ufpe.br
[2] Universidade Federal de Pernambuco – UFPE, Recife, PE, Brazil. rodrigo.qmiranda@gmail.com
[3] Universidade Federal de Pernambuco – UFPE, Recife, PE, Brazil. gabriel.antonios@ufpe.br
[4] Empresa Brasileira de Pesquisa Agropecuária – EMBRAPA Agroindústria Tropical, Fortaleza, CE, Brazil. magna.moura@embrapa.com
[5] Universidade Federal de Pernambuco – UFPE, Recife, PE, Brazil. josicleda.galvincio@ufpe.br

INTRODUCTION

Over the past twenty years, significant advances have been made in quantifying and understanding the spatio-temporal patterns of terrestrial carbon fluxes. Continuous progress in remote sensing has *played* a fundamental role in enhancing models for estimating carbon fluxes, contributing substantially to our understanding of the dynamics of carbon fluxes at local, regional, and global scales (Prakash Sarkar *et al.*, 2022; Silva, Silva, Santos, Silva, Galvíncio, 2017; Silva, Galvíncio, Silva, Soares, Tiburcio, Barros, 2024).

Arid lands cover more than 40% (Jesus *et al.*, 2023; Xue *et al.*, 2023) of the Earth's surface, encompassing several biomes that extend across approximately two-fifths of the planet, with the semi-arid domain being the most representative (Jesus *et al.*, 2023). In Brazil, the seasonally dry Brazilian tropical forest (caatinga) stands out as the fourth largest biome (Silva; Lima, Antonino; Souza; Souza; Silva; Alves, 2017; Silva; Galvíncio; Silva; Soares; Tiburcio; Barros, 2024), covering a vast area in the Northeast, approximately 912,529 km² (Tabarelli *et al.*, 2018). The environmental resilience of the caatinga is attributed to its richness in endemic species, presenting significant potential for carbon sequestration and mitigation of impacts on this ecosystem (Borges *et al.*, 2020). In the context of the caatinga, the phenological patterns of vegetation play a crucial role in regulating seasonal and annual productivity, acting as an important sink for carbon dioxide (CO_2) (Silva; Lima, Antonino; Souza; Souza; Silva; Alves, 2017; Silva; Galvíncio; Miranda; Moura, 2024).

Estimating of carbon fluxes from satellite remote-sensing products has experienced significant growth. Although the data from MOD17A2H is widely recognized, it presents potential sources of error related to both the data input and the parameters describing the biophysical properties of vegetation and the algorithm itself (Wang *et al.*, 2017).

Analyzing carbon dynamics in ecosystems over extended periods is a challenging and constantly evolving task, requiring the application of diverse datasets and simulation methods (Silva *et al.*, 2021). The integration of data from orbital sensors and ground-based sensors, capturing detailed spectral information about objects, is emerging as an essential approach for monitoring carbon storage in seasonally dry tropical forests (Silva *et al.*, 2021; Silva; Lima, Antonino; Souza; Souza; Silva; Alves, 2017).

Carbon measurement employs three main methods: direct sampling with vegetation clearing, allometric equations, and remote sensing techniques (Cerqueira; Washington Franca-Rocha, 2007; Prakash Sarkar *et al.*, 2022). Several methods are available to extrapolate information from eddy covariance (EC) flow towers, originally on a local scale, to a regional scale. These methods include statistical approaches such as regression and semi-empirical models, machine learning (ML) techniques such as neural networks and decision trees, as well as methods based on intrinsic water use efficiency models (Silva, Galvíncio, Silva, Soares, Tiburcio, Barros, 2024).

There is notable interest in the development of models aimed at monitoring environmental variables linked to the carbon balance, specifically related to Gross Primary Production (GPP), Net Ecosystem Exchange (NEE), and Ecosystem Respiration (Reco), adapted to the microclimatic characteristics of specific locations.

In the caatinga biome, there is a scarcity of precision analyses using different remote sensing methods. This research aims to explore an alternative approach to determining the carbon balance in the caatinga, utilizing remote sensing. The proposal is to develop hybrid models that combine different spectral bands, specifically from the visible and near-infrared, validated by comparing them with Reco, NEE, and GPP derived from EC carbon flux measurements in a caatinga ecosystem, aiming to facilitate the analysis of climatic conditions in seasonally dry forest areas. The underlying hypothesis seeks to evaluate the accuracy of monitoring the carbon balance in Caatinga vegetation through models calibrated for seasonally dry tropical forests, integrating field data and information from multispectral and hyperspectral orbital images.

MATERIALS AND METHODS

Characterization of the Study Area

The study area comprises the caatinga, a seasonally dry tropical forest, located in the Municipality of Petrolina, PE, Brazil. The highlighted point (Figure 1) corresponds to a legal reserve area at Embrapa Semiarid, where an eddy covariance system is installed. The vegetation in this area consists of medium and low woody formations, thorny species with small and thin leaves, cacti, and bromeliads (Kiill, 2017). The average canopy height is 4.5 meters

(Miranda *et al.*, 2020). The climate is classified as semi-arid BSh according to the Köppen classification (Alvares *et al.*, 2013), with the rainy season occurring between January and April, an average annual rainfall of 578 mm, and an average annual temperature of 26.0°C (Moura *et al.*, 2007).

Figure 1 - Seasonally Dry Tropical Forest – Caatinga, Western Pernambuco State, Petrolina, Brazil.

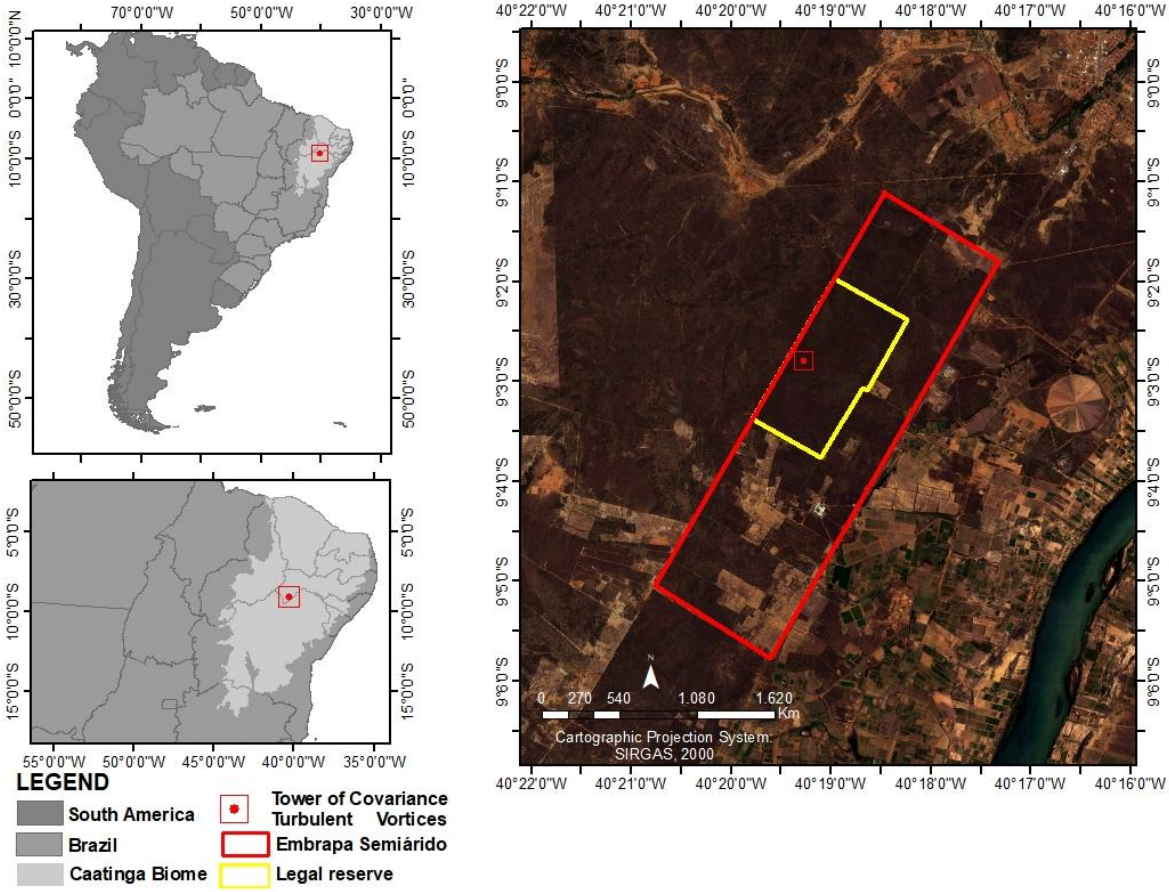

Source: IBGE (2000). Elaborated by the authors (2024).

Obtaining Data from the Flow Tower

Net Ecosystem Exchange (NEE) was calculated at 30-minute intervals using EddyPro software, version 3.6, from raw data measured at 10 Hz. Gross Primary Production (GPP) was estimated by partitioning the Net Ecosystem Exchange (NEE) into Ecosystem Respiration (Reco), following Equations 1, 2, and 3. The nighttime method was adopted to estimate Reco (Lloyd; Taylor, 1994; Reichstein *et al.*, 2005) (Equation 2). This procedure, along with gap filling, was performed using the REddyProc package in the R environment (The R Foundation, 2018). All data used pertain to the year 2015 and served as the basis for the creation and calibration of the models developed in this study. The partitioning of NEE between GPP and Reco was conducted according to Equation 1:

$$NEE = GPP - Reco \quad (1)$$

NEE is net carbon flux (µmolCO_2 m^{-2} s^{-1}), GPP is gross primary production (µmolCO_2 m^{-2} s^{-1}), and Reco is ecosystem respiration (µmolCO_2 m^{-2} s^{-1}).

$$Reco = Rref\ EE0\left(\frac{1}{Tref - T0} - \frac{1}{T - T0}\right) \quad (2)$$

Reco is the ecosystem's respiration, Tref is the reference temperature (C°), Tsoil is the soil temperature at a depth of 5 cm and T0 is a constant equal to 46.02 °C, according to Lloyd and Taylor (1994).

$$GPP = NEE - Reco \quad (3)$$

GPP is gross primary production (µmolCO_2 m^{-2} s^{-1}), NEE is net carbon flux (µmolCO_2 m^{-2} s^{-1}), and Reco is ecosystem respiration (µmolCO_2 m^{-2} s^{-1}).

Obtaining and Preprocessing Hyperspectral Data

Radiometric measurements of plant canopies were collected from January to August 2015 on random days, selecting dates close to the observed records of carbon fluxes from the micrometeorological tower, on twelve occasions during the analyzed period.

Spectral reflectance measurements were taken approximately 10 meters above the ground, in four directions (North, South, East, and West), around the EC tower. On each date and sampling area, four readings were taken, and the arithmetic mean for each collection was calculated. In this study, reflectance data obtained with HandHeld, similar to the wavelength of MOD09GA, was preferentially used for each visible and near-infrared band. The tower pixel was used to extract the reflectance of MOD09GA.

Obtaining and Processing Orbital Images

Earth surface reflectance data (MOD09GA) were used in the research, involving twelve scenes during the analyzed period. The analyses were conducted on the pixel that encompasses the tower equipped with the eddy covariance system, as the pixel was entirely contained within the preserved caatinga area.

Eight-day MOD09GA pixel values were represented by reflectance, with pixels having optimal viewing angles and minimal cloud or cloud shadow impacts selected. The extracted time series were subjected to Quality Assurance/Quality Control (QA/QC) to ensure the quality of the MOD09GA product.

MOD09GA consists of seven bands with daily resolution, presenting surface reflectance values with 500 m spatial resolution in visible (ρ_1= 620–670 nm; ρ_3= 459–479 nm; ρ_4= 545–565 nm), near-infrared (ρ_2= 841– 876 nm; ρ_5= 1230–1250 nm), and mid-infrared (ρ_6= 1628–1652 nm; ρ_7= 2105–2155 nm).

Calibration and Validation of Reco, NEE, and GPP Models

Estimates of carbon fluxes derived from the spectral bands of the FieldSpec HandHeld portable spectroradiometer were created using statistical methods. Initially, descriptive statistics were calculated, including mean, median, and standard deviation, for each developed model. Additionally, correlation and multiple linear regression analyses were conducted to establish the models, considering spectroradiometer reflectances and carbon fluxes from the Turbulent Vortex Covariance tower.

Multiple Linear Regression Model

Multiple linear regression analyses (Equation 4) were conducted using SPSS® software.

$$Y = \alpha + \beta_1 X_1 + \beta_2 X_2 + \cdots + \beta_n X_n \quad (4)$$

The models resulting from the multiple linear regression were defined by the spectral variables and carbon fluxes derived from the micrometeorological tower (Table 1). The correlation was obtained using a significance level of 0.05, i.e., 95% reliability.

Table 1 - Variables included in the model to estimate the exchange rate of carbon dioxide in micromoles of CO_2 per square meter per second (µmol CO_2 m^{-2} s^{-1}).

Variables dependents	Variables independent
Reco	ρ 550 (Green-Green)
	ρ 775 (Near Infrared - NIR)
SEN	ρ 470 (Blue)
	ρ 775 (Near Infrared - NIR)
	Reco
GPP	ρ 470 (Blue – Blue)
	ρ 775 (Near Infrared – NIR)
	SEN
	Reco

Source: The authors (2024).

Durbin-Watson Test

The multiple linear regression models were adjusted based on the analysis of the applicability of the Durbin-Watson (DW) test (Equation 5) to evaluate the presence of autocorrelation in the residuals and to ensure the independence of errors. If the DW value is greater than the upper limit, there is no autocorrelation; if it is less than the lower limit,

there is positive autocorrelation; and if it is between the two limits, the test is inconclusive. Additionally, the normality of the distribution of errors was verified through the probability of the expected value.

The Durbin-Watson (d) statistical value is given by the formula presented in Equation 5:

$$d = \frac{\sum_{i=2}^{n} \{ei-(ei-1)\}^2}{\sum_{i=1}^{n} e_i^2} \quad (5)$$

Variance Inflation Factor

The Variance Inflation Factor (VIF) was used to detect multicollinearity in the regression model (Equation 6).

$$FIV = \frac{1}{1-R_i^2} \quad (6)$$

The VIF is calculated for each independent variable, and a high score indicates high multicollinearity, which can impair the precision of the estimated regression coefficients. Values greater than 10 are often considered indicative of problematic multicollinearity.

Kappa Index

The reliability of the results obtained in this study was analyzed using the Kappa Index value ranges proposed by Landis and Koch (1977). These ranges are described in Equation 7 and are widely used to evaluate the agreement between observed data and predicted data.

$$Kappa = \frac{N*(\sum_{i=1}^{r} xii)-\sum_{i=1}^{r}(x_{i+}*x_{+i})}{N^2-\sum_{i=1}^{r}(x_{i+}*x_{+i})} \quad (7)$$

The Kappa Index, a measure of statistical agreement between actual and predicted observations, ranges from 0 to 1. The closer the Kappa Index value is to 1, the greater the accuracy of the forecast in relation to the observed data.

RESULTS AND DISCUSSION

Based on statistical criteria, the spectral variables that presented the best correlation with the model were chosen, for Ecosystem Respiration (Reco), Net Ecosystem Flow (NEE) and Gross Primary Productivity. Regression analyzes using different spectral bands (Blue, Green, Red and Near Infrared - NIR) were used to estimate Reco, NEE and GPP.

Several studies have utilized linear regression to evaluate Reco, NEE, and GPP. For instance, Li *et al.* (2016) conducted multiple linear regression analyses with optimized parameter sets to generate estimates of GPP, Reco, and NEE. Chu *et al.* (2018) investigated the distribution of precipitation and its impacts on NEE using linear regression. Zhang *et al.* (2019) evaluated ecosystem photosynthetic performance during three periods of extreme drought in a semi-arid steppe in Mongolia, applying GPP to standardize several linear regression models.

Multiple Linear Regression Model for Reco Estimation

According to the criteria selected for creating the Reco model, the most effective result was achieved by incorporating information from two spectral bands, ρ550 (Green) and ρ775 (Near Infrared - NIR), as shown in Table 2. This approach facilitated a better understanding and prediction of Reco. Notably, the average ecosystem respiration in 2015 was 1.91 µmolCO_2 m^{-2} s^{-1}, with reflectance percentages in green and infrared being 8% and 22%, respectively (Table 2). Similar results were observed in the study by Flores-Rentería *et al.* (2023), which investigated how environmental factors affect CO2 exchange throughout the year in the Chihuahuan Desert, Northeast Mexico, using the eddy covariance technique. The annual average of Reco was 1.45 µmolCO_2 m^{-2} s^{-1}. Models based on surface reflectance were developed to enhance the understanding of Reco at various sites using spectral indices (Lees *et al.*, 2018). Jägermeyr *et al.* (2014) created a Reco model using MODIS land surface temperature (LST) and the enhanced vegetation index (EVI), incorporating NIR reflectance. Wu *et al.* (2014) utilized MODIS-derived NDVI and LST (both daytime and nighttime LST) to explain Reco variations.

Table 2 - Descriptive statistics of the spectral bands ρ550 and ρ775, together with Ecosystem Respiration - Reco (in $\mu molCO_2\ m^{-2}\ s^{-1}$), derived from turbulent eddies in the variance tower and canopy reflectance measurements in the preserved Caatinga area of Petrolina - PE, in 2015.

Parameter	Average	Standard deviation	N
Reco	1.91	1.19	15
ρ550	0.0848	0.03754	15
ρ 775	0.2268	0.07618	15

Source: The authors (2024).

In this specific model, the correlation coefficient reached a significant value, with r = 0.75 and r^2 = 0.56, demonstrating statistical significance below 0.05. These results underscore the substantial association between the dependent variable Reco and the independent variables ρ550 and ρ775, as detailed in Table 3.

Table 3 - Statistical parameters of multiple linear regression for the Reco model (in $\mu molCO_2\ m^{-2}\ s^{-1}$), derived from the turbulent vortex covariance method for a preserved Caatinga area in Petrolina - PE.

Model	R	R square	Adjusted R-squared	Standard error of the estimate	R square change	Amendment F	Sig. Amendment F	Durbin - Watson	kappa
1	0.75	0.56	0.49	0.81	0.56	0.56	0.05	1,347	0.25

Source: The authors (2024).

The Reco model presented a standard error of 0.81$\mu molCO_2\ m^{-2}\ s^{-1}$, indicating a high magnitude of error. The Durbin-Watson test result of 1.347 $\mu molCO_2\ m^{-2}\ s^{-1}$ signals positive autocorrelation. Low VIF values (Variance Inflation Factor) of 1.94 suggest the possibility of overfitting, with some variability in the relationships between the variables considered acceptable, given their proximity to 2 in the 95% confidence interval. However, the absence of multicollinearity was evidenced by a tolerance of 0.51 (Table 4), and the Kappa index was 0.25, indicating weak agreement and suggesting the need for new calibrations.

There are significantly fewer successful Reco models compared to GPP due to the greater difficulty in explaining variations between ecosystems, especially using remote sensing (Jägermeyr *et al.*, 2014; Lees *et al.*, 2018).

Table 4 - Coefficients and adjustment indicators of ρ550 and ρ775 of the Reco model developed to estimate ecosystem respiration (Reco) in the Caatinga.

Model		Coefficients	95.0% Confidence Interval for B		Collinearity Statistics	
			Inferior limit	Upper limit	Tolerance	VIF
1	(Constant)	1,336	-0.154	2,827		
	ρ 550	-30.631	-48.243	-13.020	0.516	1,940
	ρ 775	13,913	5,236	22,590	0.516	1,940

Source: The authors (2024).

The predicted value for each observation is the intercept value, where the constant is 1.336, plus the regression coefficient of ρ550, which is -30.631 multiplied by the value of the independent variable, and the regression coefficient of ρ775, which is 13.913 multiplied by the value of the independent variable. The final model developed in this study to estimate Reco ($\mu molCO_2\ m^{-2}\ s^{-1}$) is as follows:

$$Reco = 1.336 + (-30.631) \times \rho\,550 + 13.913 \times \rho\,775 \quad (8)$$

Where, ρ 550 (green) and ρ 775 (Near Infrared – NIR) are the reflectances in the 550 nm and 775 nm bands, respectively.

Temporal Variability of Daily Average Reco

The assessment of Ecosystem Respiration (Reco) was based on the comparison of turbulent vortex data measured in the preserved Caatinga area throughout 2015. Reco measured by the Turbulent Vortex System (EC) presented an

average of 1.91µmolCO_2 m $^{-2}$ s $^{-1}$, while the Reco model developed and applied to data from the MOD09GA sensor (Model Developed/MOD09GA) for the same year recorded an average of 2.06 µmolCO_2 m $^{-2}$ s $^{-1}$. This represents approximately 93% accuracy in the average estimated value compared to the observed value at the EC tower. These results indicate the accuracy of the developed model when applied to MODIS data.

In 2015, low rainfall indicated restrictions on the respiration of semi-arid ecosystems due to water scarcity, limiting Reco (Figure 2) (Jia *et al.*, 2020). Global studies have highlighted the impacts of reduced precipitation, showing a weak or absent seasonal correlation with Reco (Gao *et al.*, 2015; Jia *et al.*, 2020; Zhou *et al.*, 2020). The model developed in this study demonstrated effectiveness in dealing with dry ecosystems and periods of reduced precipitation.

The seasonal Ecosystem Respiration (Reco) curves showed similar patterns during most of the analyzed period (Figure 2), comparing values observed in the tower with estimates from the model applied to MODIS data. The proximity was notable during the dry period, whereas there was divergence during the rainy period, notably around the precipitation peak between March 20 and April 17. Minimal rainfall can stimulate the release of CO_2, especially through microbial respiration (Gao *et al.*, 2015; Jia *et al.*, 2020; Sun *et al.*, 2020). During more intense water deficits, plant transpiration is reduced, leading to decreased photosynthesis, loss of canopy cover, and increased exposure to radiation and insolation. These conditions result in significant temperature variations, reduced humidity, and increased microbial activity, contributing to CO2 loss.

Figure 2 - Temporal variation of Ecosystem Respiration (Reco) derived from the turbulent vortex system and the developed model applied to data from the MOD09GA sensor (Developed Model/MOD09GA), along with rainfall records.

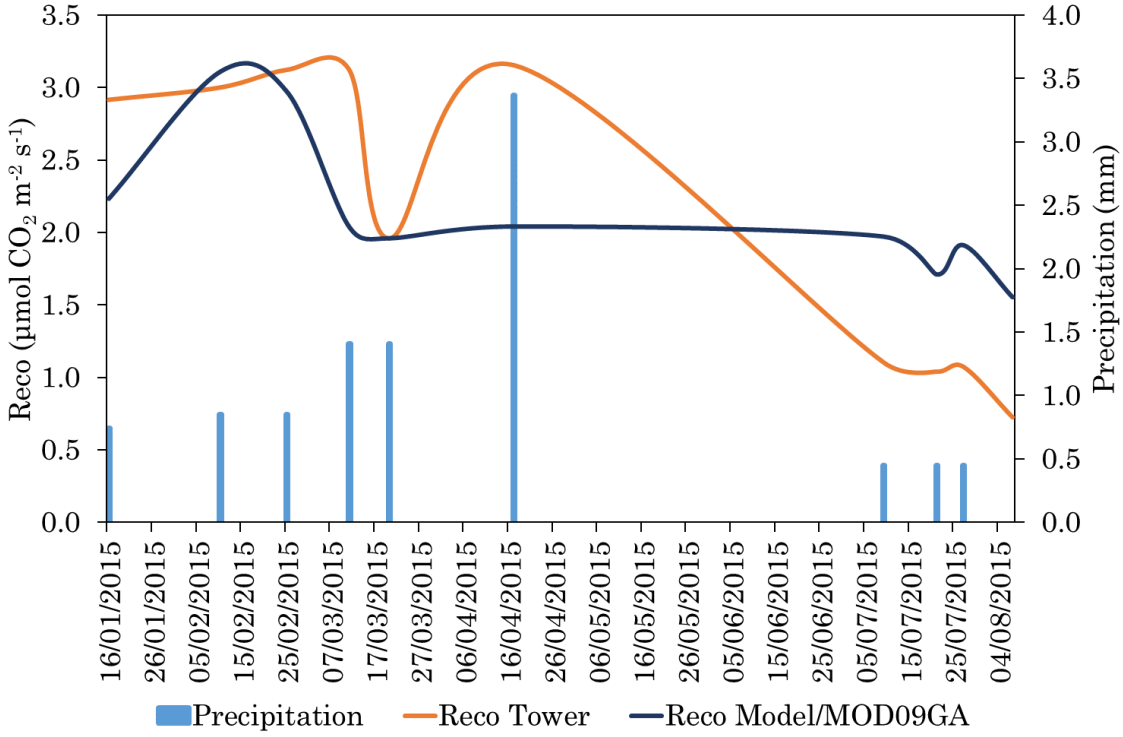

Source: The authors (2024).

The Reco of the developed model/MOD09GA did not follow the precipitation curve, indicating that this model requires further calibrations. However, given the absence of Reco models calibrated for the Caatinga vegetation using orbital images, this model can be utilized in the absence of a better-calibrated model for this vegetation. Statistical analyses revealed that it is feasible to estimate ecosystem respiration with considerable precision using reflectance data from the visible range. Therefore, the model developed in this study plays a significant role in the spatial and temporal assessment of ecosystem respiration in tropical dry forests.

Figure 3 - Simple Linear Regression between Ecosystem Respiration (Reco) derived from the turbulent vortex system and Reco from the developed model/MOD09GA.

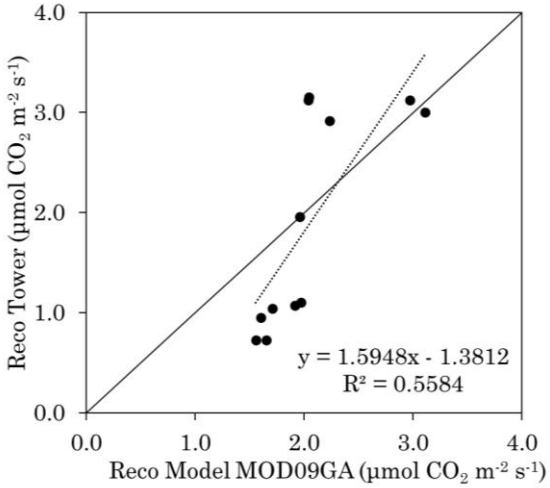

Source: The authors (2024).

The validation of the model developed in this study, using MODIS data, revealed statistical significance ($p < 0.04$) and a coefficient of determination of 0.5584 (Figure 3). The data is well-distributed along the trend line, indicating a tendency towards overestimation in relation to the tower data, mainly for < 2.0 $\mu molCO_2\ m^{-2}\ s^{-1}$ values.

This overestimation by MODIS may be associated with its spatial resolution, which represents the average of a 500-meter pixel. The Reco Model Developed/MOD09GA proved to be more reliable, although it overestimated the values in both the rainy and dry seasons, capturing the seasonality of precipitation in the study area efficiently.

It is important to highlight the scarcity of observed or estimated Ecosystem Respiration (Reco) data through remote sensing. While there are several models for estimating Gross Primary Production (GPP) using orbital sensors, there is limited availability of similar methods for estimating Reco, particularly for Caatinga vegetation.

Multiple linear regression model for estimating NEE

After several attempts to create the Net Ecosystem Exchange (NEE) model, the most effective result was achieved using two spectral bands, ρ470 (Blue) and ρ775 (Near Infrared - NIR), along with Reco (Table 5). The average net ecosystem flux for 2015 was 1.66 $\mu molCO_2\ m^{-2}\ s^{-1}$, with reflectance in the blue band at 0.06% and in the infrared band at 22% (Table 5).

Table 5 – Descriptive Statistics of the NEE Model Data, from the Spectral Bands ρ470, ρ775, and the Reco $\mu molCO_2\ m^{-2}\ s^{-1}$ fluxes derived from Turbulent Vortices and Reflectance Measured in the Canopy in the Preserved Caatinga Area in Petrolina - PE, in 2015.

Parameter	Average	Detour Standard	N
NEE	1.6605	0.43361	14
ρ470	0.0601	0.03481	14
ρ775	0.2246	0.07860	14
Reco	1.9100	1.19017	14

Source: The authors (2024).

The model presented a correlation coefficient of $r = 0.36$ and $r^2 = 0.13$, with a significance level below 0.05. These results reflect the degree of association between the dependent variable Reco and the independent variables ρ470 and ρ775. The Kappa index was 0.65, indicating moderate agreement (Table 6).

Table 6 - Statistical Parameters of Multiple Linear Regression for Developing the NEE Model ($\mu molCO_2\ m^{-2}\ s^{-1}$) derived from the Turbulent Vortex Covariance Method for a preserved Caatinga Area in Petrolina - PE.

Model	R	R square	Adjusted R-squared	Standard error of the estimate	R square change	Amendment F	Sig. Amendment F	Durbin - Watson	Kappa
1	0.36	0.13	0.2	0.79	0.13	0.35	0.78	2.43	0.65

Source: The authors (2024).

It is observed that the Net Ecosystem Flow (NEE) model developed demonstrates good ability to represent estimates, as indicated by the VIF, which varied between 2.4 and 3.15 (Table 7). The NEE model can represent the estimates well, since the VIF was between 2.4 and 3.15 (Table 7).

Table 7 - Coefficients and Adjustment Indicators for ρ470, ρ775, and Reco ($\mu molCO_2\ m^{-2}\ s^{-1}$) Developed to Estimate the Net Ecosystem Exchange (NEE) in the Caatinga.

Model		95.0% Confidence Interval for B		Collinearity Statistics	
	Coefficients	Inferior limit	Upper limit	Tolerance	VIF
1 (Constant)	1.611	0.831	2.392		
ρ470	13.180	2.098	24.261	0.318	3.149
ρ 775	-5.913	-10.198	-1.628	0.417	2.400
Reco	0.306	0.017	0.596	0.397	2.516

Source: The authors (2024).

The parameters and variables of the NEE model ($\mu molCO_2\ m^{-2}\ s^{-1}$) developed in this study are as follows:

$$NEE = 1.611 + 13.180 \times \rho 470 + (-5.913) \times \rho 775 + 0.306 \times Reco \quad (9)$$

Where, Reco is the ecosystem's respiration, ρ470 (blue) and ρ775 (Near Infrared – NIR) are the reflectances at wavelengths of 470 nm and 775 nm, respectively.

Temporal variability of daily average NEE

The assessment of the Net Ecosystem Exchange (NEE) was carried out by comparing data obtained from turbulent vortices in the preserved Caatinga area during 2015. Throughout the year, NEE measured by the Turbulent Vortex System presented an average of 1.6605 $\mu molCO_2\ m^{-2}\ s^{-1}$, while the regression-derived NEE model recorded an average of 1.556 $\mu molCO_2\ m^{-2}\ s^{-1}$.

The results of this study align with research in various semi-arid environments. Silva, Galvíncio, Miranda, Moura (2024) recorded NEE values of 1.4 and 3.6 $\mu molCO_2\ m^{-2}\ s^{-1}$ for pasture and Caatinga, respectively. The annual average varied between -3.25 $\mu molCO_2\ m^{-2}\ s^{-1}$ for pasture and -3.42 $\mu molCO_2\ m^{-2}\ s^{-1}$ for Caatinga.

Figure 4 - Temporal variation of the ecosystem Net Flux (NEE) derived from the turbulent vortex system and the developed model applied to data from the MOD09GA sensor (Model Developed/MOD09GA), together with rainfall records.

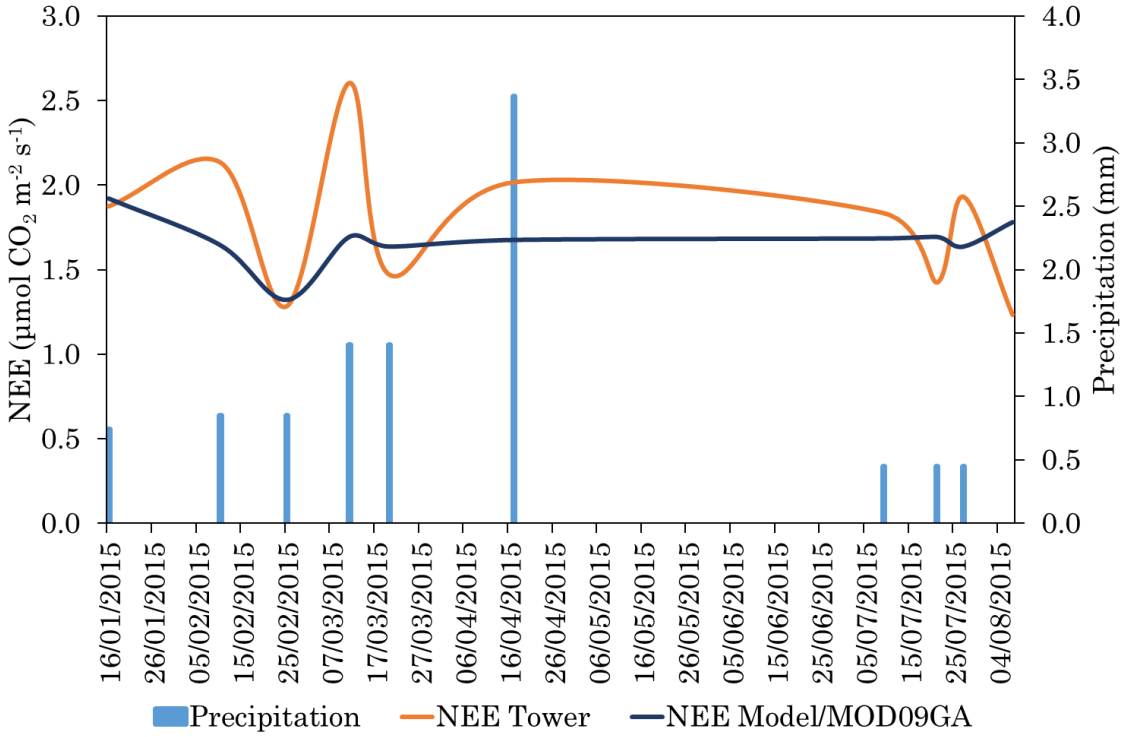

Source: The authors (2024).

The developed model presented a consistent temporal pattern for NEE, as illustrated in Figure 4. The model responds well to variations in periods of more regular rain and drought, although the extreme value measured reached a peak of 2.6 µmolCO_2 m^{-2} s^{-1}. Compared to data observed by the tower, NEE exhibited a similar seasonal pattern during most of the analyzed period. Low values were noted in a preserved fragment of Caatinga due to soil moisture deficit, impacting vegetation, as observed in previous studies (Mendes *et al.*, 2021; Pereira *et al.*, 2020; Silva; Lima; Antonino; Souza; De Souza; Silva; Alves, 2017).

The simple linear regression between the NEE from the turbulent vortex system and the NEE from the Developed Model/MOD09GA for 2015 resulted in a coefficient of determination of 0.049 (Figure 5). The data distribution along the trend line shows an overestimation in the tower's NEE model. Despite the weak statistics, it is important to highlight that, due to the absence of calibrated models for this ecosystem, the developed model may be useful until a deeper understanding is achieved (Figure 5).

Figure 5 - Simple Linear Regression between the NEE derived from the Turbulent Vortex System and the NEE derived from developed the model/MOD09GA.

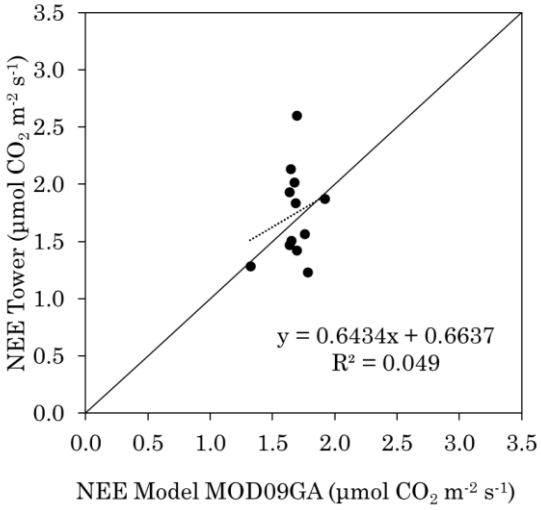

Source: The authors (2024).

Multiple linear regression model for GPP estimation

Among the tests to develop the Gross Primary Production (GPP) model, the best result was achieved using the independent variables NEE, Reco, ρ470 (Blue), and ρ775 (Near Infrared - NIR). The descriptive statistics of the input data indicate an average of 0.8998 µmolCO_2 m^{-2} s^{-1} for GPP, 1.9100 µmolCO_2 m^{-2} s^{-1} for Reco, and 1.6605 µmolCO_2 m^{-2} s^{-1} for NEE. Furthermore, the reflectance in the blue band was 6%, while in the infrared band was 22%, both referring to the year 2015 (Table 8).

Table 8 - Descriptive statistics of the GPP model data, derived from the spectral bands ρ470, ρ775 and the Reco and NEE fluxes µmolCO_2 m^{-2} s^{-1} derived from turbulent vortices and the reflectance measured in the canopy in the Preserved Caatinga Area in Petrolina.

Parameter	Average	Detour Standard	N
GPP	0.8998	0.84015	14
ρ470	0.0601	0.03481	14
ρ 775	0.2246	0.07860	14
Reco	1.9100	1.19017	14
SEN	1.6605	0.43361	14

Source: The authors (2024).

For the GPP model, a very high correlation was obtained, with r = 0.97 and r^2 = 0.95 (Table 9), and a significance level of < 0.00. The model achieved a standard error of 0.20, considered low. The Kappa index was calculated as 0.65, indicating moderate agreement between observed and predicted data (Table 9).

Table 9 - Statistical parameters of multiple linear regression for developing the GPP model (µmolCO_2 m^{-2} s^{-1}) derived from the Turbulent Vortex Covariance method for a preserved caatinga area in Petrolina - PE.

Model	R	R square	R square adjusted	Standard error of the estimate	R square change	Amendment F	Sig. Amendment F	Durbin-Watson	Kappa
1	0.97	0.95	0.94	0.20	0.95	52.4	0.00	2.43	0.64

Source: The authors (2024).

The VIF demonstrated that the model can estimate GPP very accurately, as shown in Table 10. Furthermore, no multicollinearity was identified in the model, confirming the robustness of the estimates.

The GPP model (µmolCO_2 m^{-2} s^{-1}) developed in this study was:

$$GPP = 0.284 + 1.947 \times \rho\,775 + (-5.598) \times \rho\,470 + 0.551 \times Reco + (-0.323) \times NEE \quad (10)$$

Where, ρ 470 (blue) and ρ 775 (near infrared - NIR) are the reflectances in the spectral bands of 470 nm and 775 nm, respectively.

Table 10 - Coefficients and adjustment indicators for ρ 470, ρ 775 and Reco (µmolCO_2 m^{-2} s^{-1}) of the model developed to estimate Gross Primary Productivity (GPP) in the Caatinga.

Model			95.0% Confidence Interval for B		Collinearity Statistics	
		Coefficients	Inferior limit	Upper limit	Tolerance	VIF
1	Constant	0.284	-0.530	1,098		
	ρ470	-5,598	-14.142	2,947	0.187	5,360
	ρ 775	1,947	-1.585	5,479	0.214	4,670
	Reco	0.551	0.337	0.764	0.255	3,914

Source: The authors (2024).

Temporal variability of daily GPP

The GPP was evaluated by comparing data obtained from turbulent vortices measured in the preserved Caatinga area during 2015. The GPP measured by the Turbulent Vortex System presented an average of 0.8998 µmolCO_2 m^{-2} s^{-1}, while the GPP model developed by regression demonstrated an average of 1.1380 µmolCO_2 m^{-2} s^{-1}.

Figure 6 - Temporal variation of the GPP derived from the Turbulent Vortex System and the Reco derived model applied to data from the MOD09GA sensor - Model Developed/MOD09GA and rainfall.

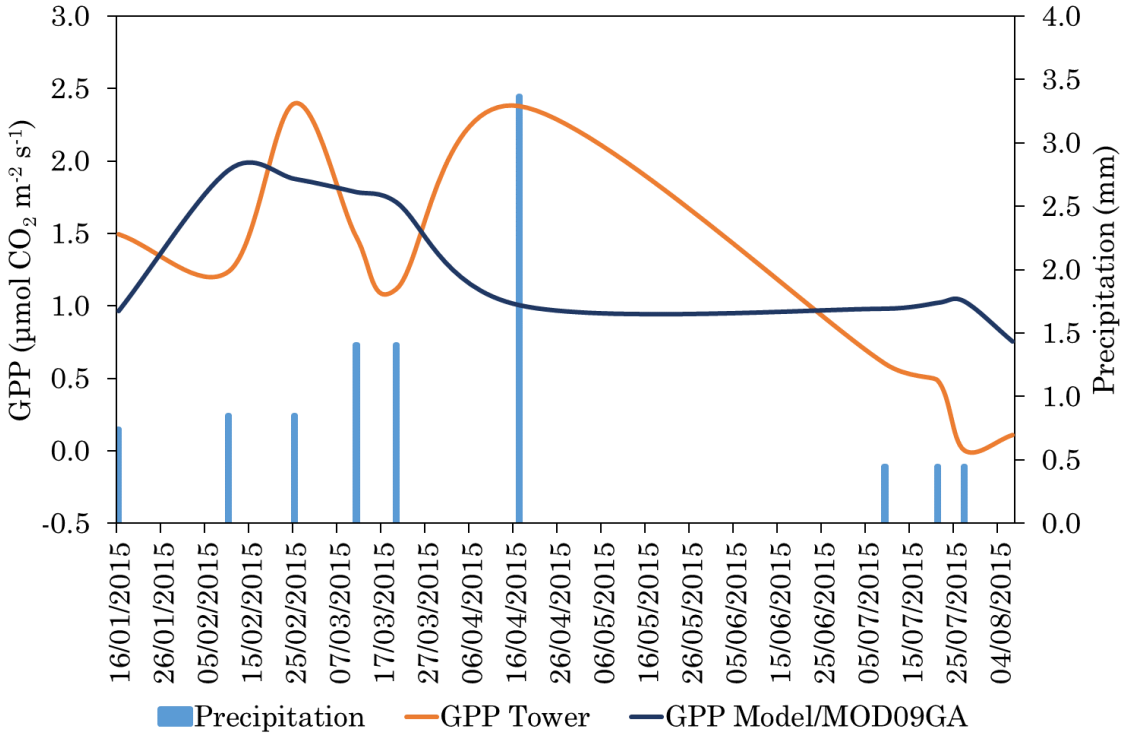

Source: The authors (2024).

GPP exhibited a similar seasonal pattern throughout most of the analyzed period. During the rainy season from January to March, the GPP of the Developed Model/MOD09GA did not follow the rains well, responding more slowly compared to the GPP of the tower, which had a faster assimilation after the rainfall from January to March. This delay in response to rainfall observed in the Developed Model/MOD09GA is consistent with studies in arid and semi-arid environments (Hao *et al.*, 2010; Liu *et al.*, 2012; Zhou *et al.*, 2020). In April, despite the increase in rainfall, the GPP estimates from the Developed Model/MOD09GA decreased, extending until June. During these months, both followed a similar seasonal pattern, but the Developed Model/MOD09GA GPP overestimated the Tower GPP. The lack of

rain during this period resulted in water stress, being the main factor for the reduction in GPP assimilation. In general, the Developed Model/MOD09GA overestimated the values in the dry season but managed to capture the seasonality of precipitation in the study area well (Figure 6).

The simple regression analysis between the GPP of the tower and the GPP of the Developed Model/MOD09GA for the year 2015 revealed a correlation coefficient of r = 0.5765 (Figure 7).

These results align with research conducted in various regions worldwide. In the study by Maselli *et al.* (2017) on Pianosa Island, a low average GPP trend (0.11 gC m^{-2} day^{-1}) was identified. Furthermore, in a study by Morais (2019) at the Embrapa Semiárido site - Brazil, the analysis of the GPP recorded by the EC during the period from 2011 to 2015 indicated an average of 1.91 ± 2.31 gC m^{-2} day^{-1}.

Figure 7 - Simple Linear Regression between Gross Primary Production - GPP derived from the Turbulent Vortex System, and Gross Primary Production - GPP derived from Model developed/MOD09GA.

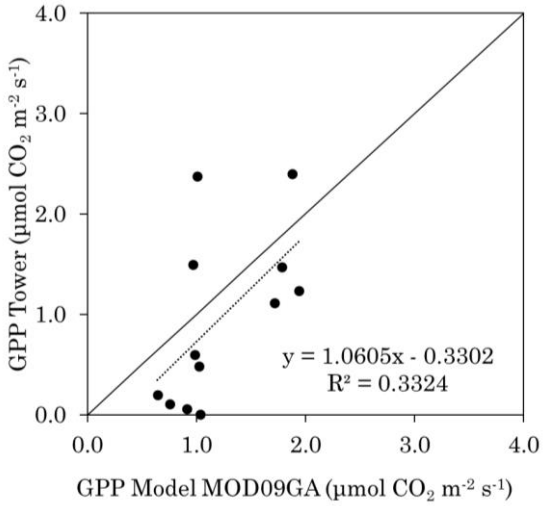

Source: The authors (2024).

When the GPP models were evaluated and compared with the reference GPP derived from the turbulent vortex system, it was observed that the model developed from *in situ reflectances* presented superior results in the seasonal pattern of the region, standing out with a presence more significant in the value of the GPP.

CONCLUSIONS

Carbon flows and ecosystem respiration in the Caatinga are essential to addressing current environmental challenges in this significant semi-arid region. This study highlights the importance of models calibrated for this specific type of vegetation and climate to accurately estimate Reco, NEE, and GPP of the Caatinga ecosystem.

The variables that showed the best correlation with the measured and observed data were those for estimating GPP and NEE. In contrast, Reco proved to be less representative, indicating the need for improvements. However, it is still feasible to consider its use in the absence of a better-calibrated Reco model.

The differences observed between the data measured by the turbulent vortex system and those estimated using the Developed Model/MOD09GA for Reco, NEE, and GPP during the rainy season, particularly in April, highlight the need to calibrate models with meteorological data. Precipitation plays a crucial role in the Caatinga's ability to capture CO2.

The use of the terrestrial and orbital data set from the MODIS/Terra sensor bands (MOD09GA) resulted in overestimation, likely due to its spatial resolution, which represents the average of a 500-meter pixel. However, the results of the models were much better than those previously available for estimates of gross primary production and respiration of dry ecosystems, especially in the Caatinga biome.

ACKNOWLEDGEMENTS

The authors would like to thank the Fundação de Amparo à Ciência e Tecnologia do Estado de Pernambuco (FACEPE) for financial assistance (process no.: IBPG-0030-9.25/18), Embrapa Semiárido for providing field data, and the Sensoriamento Remoto e Geoprocessamento Laboratory (SERGEO) and the Universidade Federal de Pernambuco (UFPE).

REFERENCES

ALVARES, C. A.; STAPE, J. L.; SENTELHAS, P. C.; DE MORAES GONÇALVES, J. L.; SPAROVEK, G. Köppen's climate classification map for Brazil. **Meteorologische Zeitschrift**, Australia, v. 22, n.6, p.711-728, 2013. https://doi.org/10.1127/0941-2948/2013/0507

BORGES, C. K.; C DOS SANTOS, C. A; CARNEIRO, R. G.; DA SILVA, L. L.; DE OLIVEIRA, G.; MARIANO, D.; SILVA, M. T.; DA SILVA, B. B.; BEZERRA, B. G.; PEREZ-MARIN, A. M.; DE MEDEIROS, S. S. **Seasonal variation of surface radiation and energy balances over two contrasting areas of the seasonally dry tropical forest (Caatinga) in the Brazilian semi-arid region,** Bethesda, v.192, p. 524 -542, 2020**.** https://doi.org/10.1007/s10661-020-08484-y

CERQUEIRA, D. B.; WASHINGTON FRANCA-ROCHA. Relationship between vegetation types and CO2 flow in the Caatinga Biome: Case study in Rio de Contas - Ba. **Proceedings XIII Brazilian Symposium on Remote Sensing,** Florianópolis**,** p. 2413–2419, 2007. Available: http://marte.dpi.inpe.br/col/dpi.inpe.br/sbsr@80/2006/11.16.00.29/doc/2413-2419.pdf . Accessed on: jul. 26, 2024.

CHU, X.; HAN, G.; XING, Q.; XIA, J.; SUN, B.; YU, J.; LI, D. Dual effect of precipitation redistribution on net ecosystem CO2 exchange of a coastal wetland in the Yellow River Delta. **Agricultural and Forest Meteorology**, Guelph, v. 249, p. 286–296, 2018. https://doi.org/10.1016/j.agrformet.2017.11.002

FLORES-RENTERÍA, D.; DELGADO-BALBUENA, J.; CAMPUZANO, E. F.; CURIEL YUSTE, J. Seasonal controlling factors of CO2 exchange in a semiarid shrubland in the Chihuahuan Desert, Mexico. **Science of The Total Environment**, Amsterdam v. 858, n.3, p. 159918, 2013. https://doi.org/10.1016/J.SCITOTENV.2022.159918

GAO, Y.; YU, G.; LI, S.; YAN, H.; ZHU, X.; WANG, Q.; S.H.I, P.; ZHAO, L.; LI, Y.; ZHANG, F.; WANG, Y.; ZHANG, J. A remote sensing model to estimate ecosystem respiration in Northern China and the Tibetan Plateau. **Ecological Modelling**, Texas, v. 304, p. 34–43, 2015. https://doi.org/10.1016/j.ecolmodel.2015.03.001

HAO, Y.; WANG, Y.; MEI, X.; CUI, X. The response of ecosystem CO2 exchange to small precipitation pulses over a temperate steppe. **Plant Ecology**, v. 2, p. 335–347, 2010. https://doi.org/10.1007/S11258-010-9766-1

IBGE –INSTITUTO BRASILEIRO DE GEOGRAFIA E ESTATÍSTICA. Mapas cartográficos: IBGE, 2000. Available: https://www.ibge.gov.br/geociencias/downloads-geociencias.html. Accessed on: may 10, 2023

JÄGERMEYR, J.; GERTEN, D.; LUCHT, W.; HOSTERT, P.; MIGLIAVACCA, M.; NEMANI, R. A high-resolution approach to estimating ecosystem respiration at continental scales using operational satellite data. **Global Change Biology**, v. 20, n. 4, p. 1191–1210, 2014. https://doi.org/10.1111/gcb.12443

JESUS, J.B DE.; KUPLICH, T.M.; BARRETO, Í. D. DE C.; GAMA, D.C. Dual polarimetric decomposition in Sentinel-1 images to estimate aboveground biomass of arboreal caatinga. **Remote Sensing Applications: Society and Environment**, v. 29, p. 1-10, 2023. https://doi.org/10.1016/J.RSASE.2022.100897

JIA, X.; MU, Y.; ZHA, T.; WANG, B.; QIN, S.; TIAN, Y. Seasonal and interannual variations in ecosystem respiration in relation to temperature, moisture, and productivity in a temperate semi-arid shrubland. **Science of the Total Environment**, v. 709, p. 136210, 2020. https://doi.org/10.1016/j.scitotenv.2019.136210

KIILL, L. H. P. **Characterization of the vegetation of the Embrapa Semiarid legal reserve.** 1. Ed. Petrolina: Embrapa Semiárido, 2017. Available: https://ainfo.cnptia.embrapa.br/digital/bitstream/item/172951/1/SDC281.pdf. Accessed on: nov. 26, 2024.

LANDIS J.R.; KOCH G.G. The measurement of observer agreement for categorical data. **Biometrics**. Washington, p. 159 – 174, v. 33, n. 1, 1977. https://doi.org/10.2307/2529310

LEES, K. J.; QUAIFE, T.; ARTZ, R. R. E.; KHOMIK, M.; CLARK, J. M. Potential for using remote sensing to estimate carbon fluxes across northern peatlands – A review. In **Science of the Total Environment,** Amsterdam, v. 615, p. 857–874, 2018. https://doi.org/10.1016/j.scitotenv.2017.09.103

LI, Q.; XIA, J.; SHI, Z.; HUANG, K.; DU, Z.; LIN, G.; LUO, Y. Variation of parameters in a Flux-Based Ecosystem Model across 12 sites of terrestrial ecosystems in the conterminous USA. **Ecological Modelling**, Texas, v. 336, p. 57–69, 2016. https://doi.org/10.1016/j.ecolmodel.2016.05.016

LIU, J. F.; CHEN, S. P.; HAN, X. G. Modeling gross primary production of two steps in

Northern China using MODIS time series and climate data. **Procedia Environmental Sciences**, v. 13, p. 742–754, 2012. https://doi.org/10.1016/j.proenv.2012.01.068

LLOYD, J.; TAYLOR, J. A. On the Temperature Dependence of Soil Respiration. **Functional Ecology**, v. 8, n. 3, p. 315-323, 1994 https://doi.org/10.2307/2389824

MASELLI, F.; VACCARI, F. P.; CHIESI, M.; ROMANELLI, S.; D'ACQUI, L. P. Modeling and analyzing the water and carbon dynamics of Mediterranean macchia by the use of ground and remote sensing data. **Ecological Modeling**, v. 351, p. 1–13, 2017. https://doi.org/10.1016/j.ecolmodel.2017.02.012

MENDES, K. R.; CAMPOS, S.; MUTTI, P. R.; FERREIRA, R. R.; RAMOS, T. M.; MARQUES, T. V.; REIS, J. S.; VIEIRA, M. M DE L.; SILVA, A. C. N.; MARQUES, A. M. S.; SILVA, D. T. C., SILVA, D. F.; OLIVEIRA, C. P.; GONÇALVES, W. A.; COSTA, G. B.; POMPELLI, M. F.; MARENCO, R. A, ANTONINO, A. C. D.; MENEZES, R. S. C.; SILVA, C. M. S. E. Assessment of SITE for CO2 and Energy Fluxes Simulations in a Seasonally Dry Tropical Forest (Caatinga Ecosystem). **Forests**, v. 12, p. 86, 2021. https://doi.org/10.3390/F12010086

MIRANDA, R. Q.; NÓBREGA, R. L. B.; MOURA, M. S. B.; RAGHAVAN, S.; GALVÍNCIO, J. D. Realistic and simplified models of plant and leaf area indices for a seasonally dry tropical forest. **International Journal of Applied Earth Observation and Geoinformation**, v. 85, p. 101992, 2020. https://doi.org/10.1016/j.jag.2019.101992

MORAIS, Y. C. **Spatial and temporal variation of gross primary production in the caatinga biome**. Thesis (Doctorate in development and end environment). UFPE, 2019. Available: https://repositorio.ufpe.br/handle/123456789/33940. Accessed on: nov. 01, 2019.

MOURA, M. S. B.; GALVÍNCIO, J. D. G.; BRITO, L. T. L.; SOUZA, L. S. B.; SÁ, I. I. S.; SILVA, T. G. F. Climate and rainwater in the Semi-Arid. In: BRITO, L.T. L.; MOURA, M. S. B.; GAMA, G. F. B (org.). **Potentialities of rainwater in the Brazilian Semi-Arid.** Petrolina: Embrapa Semi-Árido, 2007. Available: https://www.alice.cnptia.embrapa.br/bitstream/doc/159649/1/OPB1515.pdf. Accessed on: dec. 15, 2022.

PEREIRA, M. P. S.; MENDES, K. R.; JUSTINO, F.; COUTO, F.; SILVA, A. S.; SILVA, D. F.; MALHADO, A. C. M. Brazilian Dry Forest (Caatinga) Response To Multiple ENSO: the role of Atlantic and Pacific Ocean. **Science of The Total Environment**, v. 705, p. 135717, 2020. https://doi.org/10.1016/j.scitotenv.2019.135717

PRAKASH. S.; D., SHANKAR, B.; RANJAN PARIDA, B. Machine learning approach to predict terrestrial gross primary productivity using topographical and remote sensing data. **Ecological Informatics**, v.*70*, p.101697, 2022. https://doi.org/10.1016/j.ecoinf.2022.101697

REICHSTEIN, M.; FALGE, E.; BALDOCCHI, D.; PAPALE, D.; AUBINET, M.; BERBIGIER, P.; BERNHOFER, C.; BUCHMANN, N.; GILMANOV, T.; GRANIER, A.; GRÜNWALD, T.; HAVRÁNKOVÁ, K.; ILVESNIEMI, H.; JANOUS, D.; KNOHL, A.; LAURILA, T.; LOHILA, A.; LOUSTAU, D.; MATTEUCCI, G.; VALENTINI, R. On the separation of net ecosystem exchange into assimilation and ecosystem respiration: review and improved algorithm. **Global Change Biology**, v. 9, n. 11, p. 1424–1439, 2005. https://doi.org/10.1111/J.1365-2486.2005.001002.X

SILVA, J. N. B.; GALVÍNCIO; J. D.; MIRANDA, R. D. Q.; MOURA, M. S. B. Temporal and spatial estimation of the performance of calibrated regression models for carbon fluxes in the Caatinga Seasonally Dry Tropical Forest area. **Revista Da Casa Da Geografia de Sobral (RCGS)**, v. 26, n. 1, p. 183–206, 2024. https://doi.org/10.35701/rcgs.v26.975

SILVA, J. N. B.; GALVÍNCIO; J. D.; MIRANDA, R. D. Q.; MOURA, M.S.B. Models of Gross Primary Productivity in seasonally dry tropical forest areas, using reflectance data from caatinga vegetation. **Brazilian Journal of Physical Geography**, v. 14, p. 3775–3784, 2021. https://doi.org/10.26848/rbgf.v14.6.p3775-3784

SILVA, J. N. B.; SILVA, J. L. B.; SANTOS, A. M.; SILVA, A. C.; GALVÍNCIO, J. D. Vegetation Index as a Subsidy in the Identification of Areas With Potential for Desertification. **Journal of Environmental Analysis and Progress,** v. 4 n. 2, p. 358–367, 2017. https://doi.org/10.24221/jeap.2.4.2017.1469.358-367

SILVA, J. N. B; GALVÍNCIO, J. D.; SILVA, J. L. B; SOARES, G. A. S; SILVA, J. F. B. Analysis of the spatial distribution of carbon fluxes in the caatinga ecosystem. **Brazilian Journal of Remote Sensing**, v. 123, p. 115–123, 2024. https://doi.org/10.5281/zenodo.11332937

SILVA, P. F; LIMA, J. R. S; ANTONINO, A. C. D, SOUZA, R.; DE SOUZA, E. S., SILVA, J. R. I; ALVES, E. M. Seasonal patterns of carbon dioxide, water and energy fluxes over the Caatinga and grassland in the semi-arid region of Brazil. **Journal of Arid Environments**, v. 147, p. 71–82, 2017. https://doi.org/10.1016/j.jaridenv.2017.09.003

SILVA, J. N. B.; GALVÍNCIO, J. D.; SILVA, J. L. B.; SOARES, G. A. S.; TIBURCIO, I. M.; BARROS, J. P. F. G. Estimates of carbon sequestration by different methods in forest ecosystems: an approach to the seasonally dry tropical forest (Caatinga). **Brazilian Journal of the Environment**, v. 93, p. 75–93, 2024. https://doi.org/10.5281/zenodo.11267197

SUN, J.; ZHOU, T. C.; LIU, M.; CHEN, Y. C.; LIU,

G. H.; XU, M.; SHI, P. L.; PENG, F.; TSUNEKAWA, A.; LIU, Y.; WANG, X. D.; DONG, S. K.; ZHANG, Y. J.; LI, Y. N. Water and heat availability are drivers of the aboveground plant carbon accumulation rate in alpine grasslands on the Tibetan Plateau. **Global Ecology and Biogeography**, v. 29, p. 50–64, 2020. https://doi.org/10.1111/geb.13006

TABARELLI, M.; LEAL, I. R.; SCARANO, F. R.; SILVA, J. M. C. Caatinga: legacy, trajectory and challenges towards sustainability. **Science and Culture,** n. 70, v. 4, p. 25–29, 2018. https://doi.org/10.21800/2317-66602018000400009

THE R FOUNDATION. **A: The R Project for Statistical Computing.** 2018. Available: https://www.r-project.org/. Accessed on: may 10, 2023.

VAIDYA, S.; SCHMIDT, M.; RAKOWSKI, P.; BONK, N.; VERCH, G.; AUGUSTIN, J.; SOMMER, M.; HOFFMANN, M. A novel robotic chamber system allowing to accurately and precisely determine spatio-temporal CO2 flux dynamics of heterogeneous croplands. **Agricultural and Forest Meteorology**, v. 296, p. 108206, 2021. https://doi.org/10.1016/j.agrformet.2020.108206

WANG, L.; ZHU, H., LIN, A.; ZOU, L.; QIN, W.; DU, Q. Evaluation of the Latest MODIS GPP Products across Multiple Biomes Using Global Eddy Covariance Flux Data. **Remote Sensing**, n. 9, v. 5, 2017. https://doi.org/10.3390/rs9050418

WU, C.; GAUMONT-GUAY, D.; ANDREW BLACK, T.; JASSAL, R. S.; XU, S.; CHEN, J. M.; GONSAMO, A. Soil respiration mapped by exclusively use of MODIS data for forest landscapes of Saskatchewan, Canada. **ISPRS Journal of Photogrammetry and Remote Sensing,** v. 94, p. 80–90, 2014. https://doi.org/10.1016/j.isprsjprs.2014.04.018

XUE, Y.; LIANG, H.; ZHANG, H.; YIN, L.; FENG, X. Quantifying the policy-driven large scale vegetation restoration effects on evapotranspiration over drylands in China. **Journal of Environmental Management**, n. 345, p. 118723, 2023. https://doi.org/10.1016/j.jenvman.2023.118723

ZHANG, X.; ZHANG, F.; QI, Y.; DENG, L.; WANG, X.; & YANG, S. New research methods for vegetation information extraction based on visible light remote sensing images from an unmanned aerial vehicle (UAV). **International Journal of Applied Earth Observation and Geoinformation**, v. 78, p. 215–226, 2019. https://doi.org/10.1016/J.JAG.2019.01.001

ZHOU, Y.; LI, X.; GAO, Y.; HE, M.; WANG, M.; WANG, Y.; ZHAO, L., LI, Y. Carbon fluxes response of an artificial sand-binding vegetation system to rainfall variation during the growing season in the Tengger Desert. **Journal of Environmental Management,** v. 266, p. 110556, 2020. https://doi.org/10.1016/j.jenvman.2020.110556

AUTHORS CONTRIBUTION

Joélia Natália Bezerra da Silva: Conceptualization, Data curation, Formal analysis, Writing – original draft, Funding acquisition.

Rodrigo de Queiroga Miranda: Formal analysis, Data curation.

Gabriel Antônio Silva Soares: Visualization

Magna Soelma Beserra de Moura: Methodology, Resources

Josiclêda Domiciano Galvíncio: Supervision, Validation.